Isotopic Composition and Fractionation of Mercury in Great Lakes Precipitation and Ambient Air

LYNNE E. GRATZ,*,† GERALD J. KEELER,† JOEL D. BLUM,‡ AND LAURA S. SHERMAN‡

Air Quality Laboratory, 1415 Washington Heights, SPH I Tower, and Department of Geological Sciences, 1100 N. University Ave., University of Michigan, Ann Arbor, Michigan 48109

Received February 3, 2010. Revised manuscript received September 8, 2010. Accepted September 9, 2010.

Atmospheric deposition is a primary pathway by which mercury (Hg) enters terrestrial and aquatic ecosystems; however, the chemical and meteorological processes that Hg undergoes from emission to deposition are not well understood. Hg stable isotope geochemistry is a growing field used to better understand Hg biogeochemical cycling. To examine the atmospheric Hg isotopic composition in the Great Lakes, precipitation and ambient vapor-phase Hg samples were collected in Chicago, IL, Holland, MI, and Dexter, MI, between April 2007 and September 2009. Precipitation samples were characterized by negative mass-dependent fractionation (MDF) (δ^{202}Hg = −0.79‰ to 0.18‰), while most vapor-phase samples displayed positive MDF (δ^{202}Hg = −0.59‰ to 0.43‰). Positive mass-independent fractionation (MIF) (Δ^{199}Hg = 0.04‰ to 0.52‰) was observed in precipitation, whereas MIF was slightly negative in vapor-phase samples (Δ^{199}Hg = −0.21‰ to 0.06‰). Significant positive MIF of ^{200}Hg up to 0.25‰ was also measured in precipitation. Such MIF of an even-mass Hg isotope has not been previously reported in natural samples. These results contrast with recent predictions of the isotopic composition of atmospheric Hg and suggest that, in addition to aqueous photoreduction, other atmospheric redox reactions and source-related processes may contribute to isotopic fractionation of atmospheric Hg.

Introduction

Mercury (Hg) is a hazardous air pollutant and toxic metal of significant environmental concern. Once Hg enters terrestrial and aquatic ecosystems, it can be converted to its organic form, methylmercury, which bioaccumulates within aquatic food webs and ultimately threatens human health through consumption of contaminated fish (*1*). It is critical to identify and understand the sources and transport mechanisms of Hg in the atmosphere in order to effectively regulate emissions and reduce the threat of Hg to sensitive ecosystems and populations.

Mercury exists in the atmosphere in three main forms: gaseous elemental Hg (Hg^0), divalent reactive gaseous Hg (RGM), and fine particulate bound Hg (Hg_p) (*2*). Hg^0 comprises more than 90% of the Hg in ambient air (*3, 4*). It has low solubility in water and consequently can be transported long distances in the atmosphere without being deposited (*2, 4*). In contrast, RGM and Hg_p are much more reactive and deposit readily, either close to sources (*5*) or upon oxidation of Hg^0 during atmospheric transport (*2, 4*). Given that Hg is a local, regional, and global pollutant, identifying the transport pathways, chemical transformations, and deposition mechanisms that Hg undergoes in the atmosphere can be challenging.

Mercury stable isotope geochemistry is a growing field used to examine Hg biogeochemical cycling. Mercury has seven stable isotopes (196, 198, 199, 200, 201, 202, and 204 amu), active redox chemistry, and an ability to form covalent bonds. It also commonly transforms between the solid, aqueous, and gas phases. Mass-dependent fractionation (MDF) of Hg has been observed experimentally during microbial reduction (*6, 7*) and dark abiotic aqueous reduction (*8*). MDF is also observed in natural materials, including hydrothermal emissions (*9*−*11*) and terrestrial and marine sediments (*12, 13*).

Recent studies demonstrate that mass-independent fractionation (MIF) of Hg isotopes can occur in natural systems. MIF of Hg isotopes has been observed during photoreduction of Hg^{2+} and photodegradation of methylmercury (*8*), as well as in peats (*14, 15*), sediments (*13*), hydrothermal waters (*11*), coal deposits (*15*), fish tissue (*8, 16*), lichens (*17*), and Arctic snow (*18*). MIF is measured as the deviation in isotopic composition from that predicted to occur due to kinetic MDF. MIF is predicted to occur either due to differences in nuclear charge radii among the isotopes caused by variability in the packing of protons and neutrons in the nucleus (nuclear volume effect) (*14, 19, 20*) or due to the influence of nuclear spin in the odd-mass isotopes on radical pair reaction rates (magnetic isotope effect) (*21*−*23*). The nuclear volume effect causes MIF of Hg isotopes during equilibrium reactions (*19*), whereas the magnetic isotope effect occurs during kinetic reactions (*21*−*23*). The nuclear volume theory predicts that MIF will be greatest for ^{199}Hg and ^{204}Hg (*19*), but also predicts MIF for ^{201}Hg and to a lesser degree for ^{200}Hg. However, because the effect of nuclear volume depends critically on the nuclear charge radii, which are not well-known for Hg isotopes, predictions of fractionation due to the nuclear volume effect are somewhat variable (*20*). In contrast, MIF due to the magnetic isotope effect can only affect the odd-mass isotopes of Hg (^{199}Hg and ^{201}Hg) (*23*). Further discussion of Hg isotopic fractionation can be found in the work of Bergquist and Blum (*24*).

Analyses to date suggest that quantification of Hg isotopic fractionation, including the magnitude and sign of MDF and MIF, may offer insight into sources of Hg to the environment (*15*) as well as the biogeochemical processes affecting Hg abundance and speciation in terrestrial and aquatic ecosystems (*8, 17, 18*). While atmospheric deposition is the dominant pathway for Hg to enter aquatic ecosystems (*25, 26*) and is therefore integral to the Hg biogeochemical cycle, Hg isotopes have only recently been directly measured in atmospheric reservoirs (*18, 27*).

The Great Lakes region was chosen for atmospheric Hg isotope measurements because sources of Hg in this region are well-identified (*28*−*32*), and elevated levels of Hg deposition to the Great Lakes have been observed in recent decades (*33*). Previous studies demonstrated the influence of major Hg sources in the Chicago/Gary urban area on Hg concentrations in Lake Michigan and in ambient air and precipitation in surrounding regions (*25, 30, 34*). However,

* Corresponding author phone: (734) 763-7714; e-mail: lgratz@umich.edu.
† Air Quality Laboratory.
‡ Department of Geological Sciences.

10.1021/es100383w

Published on Web 09/20/2010

the atmospheric processes that Hg undergoes following emission, as well as the relative contribution from specific source types to Hg deposition at given receptor locations, are not fully understood. The objective of this study was to develop methods for quantifying the Hg isotopic composition in atmospheric samples and to use these analyses to investigate the reactions and processes that Hg undergoes in the atmosphere.

Experimental Section

Site Descriptions. Precipitation samples were collected in Chicago, IL and Holland, MI from July 2007 to November 2007 and in Dexter, MI from April 2007 to November 2008 (Figure SI−S1, Supporting Information). Six ambient vapor-phase Hg samples were collected at the Dexter site between August 2007 and September 2009. One vapor-phase Hg sample was collected at the Chicago site in September 2009.

The Chicago, IL site (UOC) was ∼2 km west of Lake Michigan and in close proximity to Hg sources in the Chicago/Gary industrial region, including coal-fired utility boilers, metal smelters, and iron-steel manufacturers. The Holland, MI site (HOL) was ∼5 km inland on the eastern shore of Lake Michigan, ∼162 km northeast of Chicago. Holland was considered semirural because local point sources are much fewer in number than those surrounding the industrial Chicago site. Additionally, local sources are north and east of the Holland site and would minimally impact samples collected in Holland during southwest transport from Chicago/Gary. The Dexter, MI site (DXT) was ∼60 km west of Detroit, MI. It was previously demonstrated that because Dexter is a remote location with no major local Hg point sources, the air masses sampled at this site primarily represent background ambient air (*35, 36*).

Sample Collection. Precipitation samples were collected using a modified wet-only University of Michigan MIC-B (MIC, Thornhill, Ontario) automated precipitation collector. The sampling train described by Landis and Keeler (*37*) for daily-event wet-only precipitation collection was utilized. However, because substantially more Hg is needed for high-precision isotopic analysis than for Hg concentration analysis, the sample train was modified to collect precipitation through two borosilicate glass funnels (collection area per funnel = 191 ± 9 cm^2) into a single 2-L fluorinated polyethylene bottle. Each funnel was equipped with a glass vapor lock inside a Teflon adapter to prevent vapor-phase Hg exchange between precipitation and the surrounding air (*37*). Vapor locks were fitted with 23 cm long silicone tubes (0.48 cm i.d.) that connected to the 2-L bottle through a Y-shaped adapter on the bottle cap. Supplies and samples were prepared and handled using clean techniques in a Class-100 clean room. Funnels and vapor locks were prepared using a rigorous acid cleaning procedure (*37*). Fluorinated bottles were cleaned using a two-day soak in 2% BrCl followed by a thorough rinse in ultrapurified Milli-Q water. Lab and field blanks yielded <2 pg of Hg/bottle. Silicone tubing was rinsed extensively with ultrapure Milli-Q water before deployment in the field. Individual lengths of tubing were not used for more than one sample. Sample bottles were typically deployed for 1−2 weeks to allow for sufficient precipitation volume collection. Consequently, samples analyzed in this study represent composite rather than event samples.

Ambient vapor-phase Hg samples were collected onto gold-coated bead traps in a manner similar to previously reported methods (*25*). To collect sufficient Hg for isotopic analysis, eight traps were deployed in parallel on a PVC manifold for 2−3 days at a time. Air was pulled through the traps by a single pump at a constant flow rate of ∼1.8 lpm per trap. Quartz-fiber filters were placed on the upstream end of the traps to remove Hg_p from the air stream. The traps were heated to ∼60 °C during sampling to prevent condensation.

Sample Processing and Analysis. Following collection, precipitation samples were oxidized with 1% (v/v) BrCl and stored in a dark cold room for at least 24 h. Precipitation samples were analyzed for Hg concentration using cold vapor atomic fluorescence spectrometry (CVAFS) on a Tekran Series 2600. Of the 56 samples collected, 20 contained sufficient Hg (>8 ng) for isotopic analysis.

Prior to isotopic analysis, the Hg from each sample was isolated and concentrated into a 2% $KMnO_4$ (w/w) liquid trap. Each sample was first well-mixed and transferred to a clean 2-L Pyrex bottle. The reducing agents, consisting of 10% SnCl (w/v), 50% H_2SO_4 (w/v), and 1% NH_2OH (w/v), were mixed in a separate 2-L Pyrex bottle. The sample and reagents were introduced simultaneously onto a frosted-tip gas−liquid separator at a rate of 0.8 mL/min. The reduced $Hg^0(g)$ was transferred to 25 g of 2% $KMnO_4$ (w/w) solution by a counter-flow of Ar gas (350 mL/min). Procedural standards [NIST SRM 3133 in 1 L of 1% BrCl (v/v)] and blank solutions [1 L of 1% BrCl (v/v)] were pre-concentrated in the same manner.

Ambient vapor-phase samples were also pre-concentrated into 25 g of 2% $KMnO_4$ (w/w). The gold-coated bead traps were thermally desorbed by slowly heating each trap to 500 °C over 3 h, following the heating profile described in Sherman et al. (*18*) while an Ar gas stream (50 mL/min) transferred $Hg^0(g)$ into the 2% $KMnO_4$ solution. Procedural standards (NIST SRM 3133) and blank gold traps were processed following the same methods.

The 25 g 2% $KMnO_4$ (w/w) solutions were subsequently transferred into 8 g of 2% $KMnO_4$ (w/w) to sufficiently concentrate the Hg to ≥1 ng/g for isotopic analysis. This secondary step was necessary because concentrating the samples directly into 8 g of 2% $KMnO_4$ was found to cause significant loss of Hg. Each 25 g solution was partially reduced with NH_2OH and divided into 5 mL subsamples. Subsamples were individually reduced with 20 μL of 30% NH_2OH, 250 μL of 20% $SnCl_2$, and 250 μL of 50% H_2SO_4 and bubbled into 8 g of 2% $KMnO_4$ (w/w). The 8 g solutions were partially reduced with NH_2OH immediately prior to isotopic analysis. Procedural standards (NIST SRM 3133) were performed to emulate the transferred of Hg from 25 to 8 g of 2% $KMnO_4$. All liquid- and vapor-phase procedural standards were processed in the same manner as samples. Details of procedural standard preparation and analysis are provided in the Supporting Information along with the determination of recoveries in samples and standards.

The isotopic compositions of samples and standards were determined using multiple collector inductively coupled plasma mass spectrometry (MC-ICP-MS; Nu instruments) following previously published methods (*8, 38*). MDF is reported in delta notation (δ) with respect to the average isotopic composition of the NIST SRM 3133 bracketing standards (*38*), following eq 1:

$$\delta^X\mathrm{Hg}\ (‰) = \left([(^X\mathrm{Hg}/^{198}\mathrm{Hg})_{\mathrm{sample}}/(^X\mathrm{Hg}/^{198}\mathrm{Hg})_{\mathrm{NISTSRM133}}] - 1\right) \times 1000 \quad (1)$$

Throughout the manuscript MDF will be discussed using δ^{202}Hg (‰) (*38*). MIF is reported using capital delta notation (Δ) (*38*) as the deviation from predicted kinetic MDF according to the following equations (*38*):

$$\Delta^{199}\mathrm{Hg}\ (‰) = \delta^{199}\mathrm{Hg} - (\delta^{202}\mathrm{Hg} \times 0.252) \quad (2)$$

$$\Delta^{200}\mathrm{Hg}\ (‰) = \delta^{200}\mathrm{Hg} - (\delta^{202}\mathrm{Hg} \times 0.502) \quad (3)$$

$$\Delta^{201}\mathrm{Hg}\ (‰) = \delta^{201}\mathrm{Hg} - (\delta^{202}\mathrm{Hg} \times 0.752) \quad (4)$$

To assess the analytical uncertainty of isotopic analyses, the UM-Almadén standard (*38*) was analyzed during each

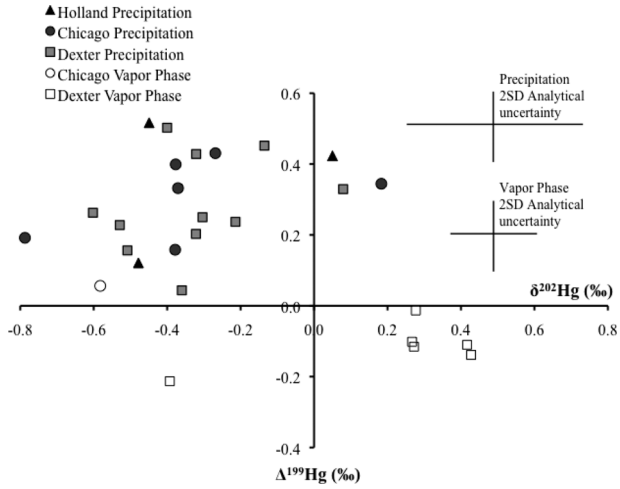

FIGURE 1. Δ^{199}Hg (‰) vs δ^{202}Hg (‰) for precipitation and ambient vapor-phase samples. Representative 2SD analytical uncertainty (0.10‰ for Δ^{199}Hg, 0.25‰ for δ^{202}Hg of precipitation, and 0.12‰ for δ^{202}Hg of vapor-phase Hg) is determined by the reproducibility of the UM-Almadén standard and procedural standards.

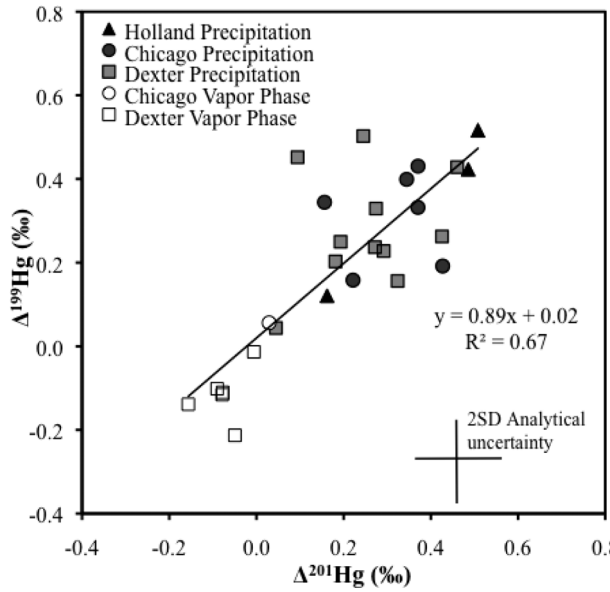

FIGURE 2. Δ^{199}Hg (‰) vs Δ^{201}Hg (‰) for precipitation and ambient vapor-phase samples. Representative 2SD analytical uncertainty (0.10‰ for Δ^{199}Hg, 0.12‰ for Δ^{201}Hg) is determined by the reproducibility of the UM-Almadén standard and procedural standards.

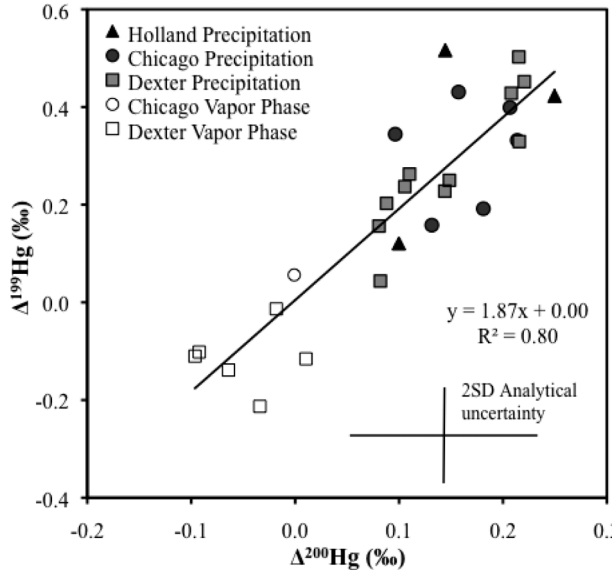

FIGURE 3. Δ^{199}Hg (‰) vs Δ^{200}Hg (‰) for precipitation and ambient vapor-phase samples. Representative 2SD analytical uncertainty (0.10‰ for Δ^{199}Hg, 0.09‰ for Δ^{200}Hg) is determined by the reproducibility of the UM-Almadén standard and procedural standards.

analytical session at concentrations comparable to sample solutions. Procedural standards (NIST SRM 3133) were also analyzed for isotopic composition. In the following discussion, analytical uncertainties are reported as the larger value of either 2SD of the reproducibility of the UM-Almadén standard or 2SD of the reproducibility of procedural standards.

Results

Figure 1 summarizes the Hg isotopic composition of Great Lakes atmospheric samples (Δ^{199}Hg versus δ^{202}Hg). Most precipitation samples were characterized by negative δ^{202}Hg (δ^{202}Hg = −0.79‰ ± 0.25‰ to 0.18‰ ± 0.25‰, 2SD), whereas δ^{202}Hg of vapor-phase samples was predominantly positive (δ^{202}Hg up to 0.43‰ ± 0.12‰, 2SD) with the exception of DXT-VP-2 (δ^{202}Hg = −0.39‰ ± 0.12‰, 2SD) and UOC-VP-1 (δ^{202}Hg = −0.59‰ ± 0.12‰, 2SD). Significant positive MIF of the odd-mass isotopes was measured in precipitation samples (Δ^{199}Hg = 0.04‰ ± 0.10‰ to 0.52‰ ± 0.10‰, 2SD; Δ^{201}Hg = 0.04‰ ± 0.12‰ to 0.51‰ ± 0.12‰, 2SD) (Figure 2). In contrast, Δ^{199}Hg and Δ^{201}Hg were either slightly negative or indistinguishable from zero in vapor-phase samples (Δ^{199}Hg = −0.21‰ ± 0.10‰ to 0.06‰ ± 0.10‰, 2SD; Δ^{201}Hg = −0.16‰ ± 0.12‰ to 0.03‰ ± 0.12‰, 2SD). A linear regression of Δ^{199}Hg versus Δ^{201}Hg for all atmospheric samples (precipitation and vapor phase) yielded a slope of 0.89 ± 0.21 ($r^2 = 0.67$, $p < 0.001$) (Figure 2).

Significant MIF of ^{200}Hg has not been reported in previous studies. However, Δ^{200}Hg was significantly different from zero in 17 of the 20 precipitation samples from this study and values up to 0.25‰ (±0.09‰, 2SD) were observed. In contrast, Δ^{200}Hg of vapor-phase samples was slightly negative but indistinguishable from zero (average Δ^{200}Hg = −0.04‰ ± 0.09‰, 2SD). A linear regression of Δ^{199}Hg versus Δ^{200}Hg in all atmospheric samples yielded a slope of 1.87 ± 0.40 ($r^2 = 0.80$, $p < 0.001$) (Figure 3). Precipitation and vapor-phase isotopic compositions are summarized in the Supporting Information (Tables SI−S1 and SI−S2).

Discussion

Ambient Sample Characterization. The range in Hg isotopic compositions of ambient vapor-phase samples suggests that Hg isotope measurements may potentially be used to distinguish between background Hg^0 and Hg emitted from industrial sources. Five of the six Dexter vapor-phase samples had similar δ^{202}Hg (‰) values within the reported 2SD analytical uncertainty. In all Dexter vapor-phase samples, Δ^{199}Hg was slightly negative (average Δ^{199}Hg = −0.12‰ ± 0.10‰, 2SD) (Figure 1). Given the rural nature of the Dexter site, these samples may represent the regional background isotopic composition of ambient vapor-phase Hg, which is predominantly Hg^0 (*3, 4, 35*). In contrast, one vapor-phase sample from Dexter (DXT-VP-2) displayed negative δ^{202}Hg (−0.39‰ ± 0.12‰, 2SD) and significant negative Δ^{199}Hg (−0.21‰ ± 0.10‰, 2SD). DXT-VP-2 was the only vapor-phase sample collected at Dexter during south−southeasterly flow. All other Dexter vapor-phase samples, with exception of DXT-VP-5, captured northerly flow. South−southeasterly flow likely transported Hg emitted from major point sources

in southeast Michigan, Ohio, and the Ohio River Valley, where coal combustion is the dominant source of atmospheric Hg (*31*) (Figure SI−S1, Supporting Information). The isotopic composition of DXT-VP-2 is similar to the measured isotopic composition of some western US coals (*15*) that are burned in the Great Lakes region (*39, 40*). The Chicago vapor-phase sample displayed similar negative δ^{202}Hg (−0.58‰ ± 0.12‰, 2SD) to DXT-VP-2. The isotopic composition of this vapor-phase sample may also be heavily influenced by the proximity of the Chicago site to many large industrial sources (e.g., coal combustion) (Figure SI−S1, Supporting Information).

Interestingly, DXT-VP-5 (δ^{202}Hg = 0.28‰ ± 0.12‰, 2SD; Δ^{199}Hg = −0.01‰ ± 0.10‰, 2SD) was collected under south−southwesterly flow but is not isotopically similar to DXT-VP-2. Although speculative, the differences between these samples may be explained by the meteorological conditions under which they were collected. During the sampling period for DXT-VP-2 (2/23/09 to 2/25/09) the average boundary layer height at Dexter was 236 m above ground level (AGL), as determined from HYSPLIT V4.8 modeled mixed layer depths at the sampling location (*41*). The average hourly ambient temperature in Dexter was −5 °C (*42*), and the sky was 60−100% obscured by clouds (*43*). Given the low boundary layer and cold temperatures, vertical mixing was limited during collection of DXT-VP-2. Additionally, the cloud cover may have reflected incoming radiation and reduced photochemical activity. In contrast, during the collection of DXT-VP-5 (5/20/09 to 5/22/09), the average hourly temperature was 20 °C (*42*), the average boundary layer depth was ∼450 m AGL with daytime heights above 1000 m AGL, and the sky was clear with few scattered clouds (*43*). Consequently, the potential for vertical mixing of point source emissions and photochemical activity during collection of DXT-VP-5 was much greater than for DXT-VP-2. It is therefore possible that DXT-VP-2 more strongly retained the isotopic signature imparted by regional coal combustion. Additional sampling of the emissions from different source types, shorter duration sampling of ambient Hg under different flow regimes, and ambient speciated measurements are needed to fully evaluate this hypothesis.

Precipitation Sample Characterization. It is difficult to characterize the meteorological history of the precipitation samples because each sample was a composite of up to six discrete events. Each event may have had unique synoptic conditions leading to the formation of precipitation and different sources of Hg emitting into the associated air mass. Previous studies clearly demonstrate that event-based sampling is essential to distinctly characterize air mass transport and deposition using meteorological data, modeled air mass back-trajectories, and trace element concentrations in precipitation (*5, 44−46*). When multiple events are combined into a single sample, it is very difficult, and perhaps no longer possible, to separate and identify specific source emission signatures. Despite these limitations, the data presented here do offer new insights into atmospheric processes and highlight important reaction mechanisms that need further examination.

Given that vapor-phase and wet-deposited Hg samples were not collected concurrently, it is not possible to draw direct relationships between them, and their contrasting isotopic signatures could be partly due to differences in sampling periods. However, it is important to consider that ambient vapor-phase Hg is predominantly Hg^0 while Hg in precipitation is primarily RGM and Hg_p. Therefore, the apparent isotopic differences between sample types may suggest that atmospheric redox reactions, which convert Hg between its elemental and oxidized forms, influence the isotopic composition of Hg in these samples.

Mass-Independent Fractionation Mechanisms. The precise mechanism(s) causing MIF of Hg isotopes are not fully understood, but previous work suggests that significant MIF can occur due to the magnetic isotope effect (*8, 14, 17, 18*). This effect occurs during photochemical reactions in which long-lived radical pairs are formed. Differences in magnetic moments and nuclear spin between even- and odd-mass isotopes can cause varying radical pair recombination rates among the isotopes and consequently alter the isotopic composition of reaction products (*8, 22, 23*). In contrast, the nuclear volume effect can occur during dark and light reactions, but the extent of fractionation is expected to be much smaller (*47*). Several Hg redox reactions occur in the atmosphere and, depending on the reaction, it is plausible that either effect might influence the isotopic composition of atmospheric Hg. It is also possible that other currently unidentified mechanisms contribute to Hg isotopic fractionation in the atmosphere.

Previous studies of MIF in natural systems suggest that the magnetic isotope effect may produce a Δ^{199}Hg/Δ^{201}Hg ratio of ∼1:1 (*8, 14, 17, 18*). The nuclear volume effect theoretically produces a Δ^{199}Hg/Δ^{201}Hg ratio of ∼2.5:1 (*14, 19, 20*). The Δ^{199}Hg/Δ^{201}Hg ratio in precipitation and vapor-phase Hg samples (Figure 2) is similar to the ratio suggested to occur due to the magnetic isotope effect and is indistinguishable from 1:1. However, variability in Δ^{199}Hg/Δ^{201}Hg ratios for individual samples may suggest that more than one reaction and/or mechanism is causing the observed MIF.

Comparison of Results to Previous Studies. The observed positive MIF of ^{199}Hg and ^{201}Hg in precipitation and mostly insignificant MIF of ^{199}Hg and ^{201}Hg in ambient vapor-phase samples are in contrast to previous studies that suggested atmospheric Hg should display significant negative MIF (*17*). During aqueous photoreduction experiments by Bergquist and Blum (*8*), Hg^0(g) was volatilized from solutions containing dissolved organic carbon (DOC) and the Hg^{2+} remaining in solution displayed increasingly positive Δ^{199}Hg and Δ^{201}Hg. It was therefore hypothesized that Hg^0(g) released to the atmosphere through aqueous photoreduction should display negative MIF (*8*). Additionally, a recent study reported negative MIF of Hg in lichens from Switzerland, northeast France, and northern Quebec, Canada, where Δ^{199}Hg and Δ^{201}Hg values between −1.0‰ and −0.3‰ (±0.15‰, 2SD) were observed (*17*). Because lichens take up Hg through wet and dry deposition (including possible direct absorption of atmospheric Hg^0), it was suggested that the Hg isotopic composition of lichens might represent the isotopic values of atmospheric Hg (*17*). It was further suggested that the atmosphere and aquatic environment may be complementary reservoirs with respect to photoreduction of Hg and that aqueous photoreduction may be the dominant process influencing atmospheric Hg (*17*). However, we suggest that aqueous photoreduction in the presence of DOC is not the only process contributing to the isotopic composition of Hg in the atmosphere.

The sources and processes relevant to atmospheric Hg cycling vary on local and regional scales due to the density of sources, the speciation and quantity of emissions, and the concentrations of other atmospheric constituents. Therefore, the dominant processes influencing Hg isotopic fractionation should be examined carefully for each location of interest. The isotopic composition of Hg^0 released during aqueous photoreduction is not necessarily the same as the isotopic composition of Hg released from anthropogenic sources or the isotopic composition of Hg produced via other reaction mechanisms. Although aqueous photoreduction is a potential source of atmospheric Hg^0 in the Lake Michigan Basin, the high density of industrial sources in the region as well as post-emission atmospheric processes would also likely influence the isotopic composition of atmospheric Hg.

Mercury can undergo a wide range of gas-phase, aqueous-phase, and heterogeneous reactions between emission and deposition. For example, Hg^0 can be oxidized in the gas and aqueous phases by hydroxyl radicals, ozone, and halogen compounds (*48*−*50*). Reduction of Hg^{2+} can occur in the aqueous phase by sulfite, halogen species, or hydroperoxyl radicals (*4, 50, 51*). Photoreduction can also occur in the atmosphere during heterogeneous reactions in cloud droplets (*49, 52*) and within power plant plumes (*53*).

The importance of heterogeneous chemistry in Hg isotopic fractionation was recently demonstrated in Arctic snow samples. Following photochemical reduction of Hg^{2+} in surface snow through reactions likely involving Hg−halogen radical pair intermediates, Δ^{199}Hg in the surface snow decreased significantly (<−4‰) while the emitted Hg^0(g) displayed less negative Δ^{199}Hg values than the original surface snow (*18*). These findings highlight the importance of photochemistry to Hg isotopic fractionation. It is plausible that Hg fractionation in the atmosphere might occur during similar processes. Halogen reactions are typically important in Arctic environments (*54, 55*) and the marine boundary layer (*56, 57*). In the industrial Great Lakes region, ozone is more readily available (*58*) and therefore may dominate Hg^0 oxidation (*59*). However, there are also important industrial halogen sources in the Great Lakes region, such as municipal solid waste incinerators (*60*), which could contribute to Hg^0 oxidation.

Photoreduction in cloud droplets may facilitate the release of Hg^0 back to the interstitial air. Cloud droplets contain some DOC (*61, 62*), and if experiments conducted by Bergquist and Blum (*8*) are relevant to this system, then during photoreduction the odd-mass isotopes of Hg would be preferentially retained as Hg^{2+} in the cloud droplet. Consequently, cloud droplets would become increasingly positive with respect to Δ^{199}Hg. Oxidation reactions in the atmosphere could also cause MIF of Hg isotopes. However, because oxidation by ozone or halogen radicals is not a direct photochemical process and thus does not produce long-lived radical pairs, it is unlikely that this process produces significant MIF of Hg isotopes (*22, 47*). The possible mechanisms and full range of reactions responsible for MIF of Hg in the atmosphere should be examined more closely under carefully controlled experimental conditions.

Mass-Independent Fractionation of ^{200}Hg. Significant MIF of ^{200}Hg was observed in precipitation and vapor-phase Hg samples. Such MIF of an even-mass Hg isotope has not been previously reported in natural samples. Although Δ^{200}Hg observed in atmospheric samples is relatively small, the values are larger than the 2SD uncertainty (0.09‰) in all but three precipitation samples. A consistent pattern between Δ^{200}Hg and Δ^{199}Hg is also evident (Figure 3). There is no indication that this MIF is the result of instrumental artifacts, and procedural standards and blanks did not display significant Δ^{200}Hg. Because the even-mass Hg isotopes do not have nuclear magnetic moments or nuclear spin, MIF of ^{200}Hg cannot be caused by the magnetic isotope effect (*21, 23*). The nuclear volume effect could cause slight MIF of the even Hg isotopes, but estimates of the magnitude of this effect suggest that it should not be detectable (*19*). However, given the uncertainty in nuclear charge radii for Hg isotopes, the effect of nuclear volume on ^{200}Hg may not be accurately characterized at this time. There are other mechanisms, such as photochemical self-shielding (*63*), which have not yet been extensively explored that could potentially cause MIF of even-mass Hg isotopes. It should be noted that because Δ values are calculated with respect to the ^{202}Hg/^{198}Hg ratio, by definition MIF of ^{198}Hg would not be detected. Therefore, the MIF observed for ^{200}Hg could involve fractionation of ^{198}Hg, ^{200}Hg, or ^{202}Hg.

Implications. The results of this study demonstrate that the isotopic composition of Hg can be measured with high precision in atmospheric samples. We suggest that MIF of atmospheric Hg may be caused by a combination of source emissions and complex atmospheric reactions. Although specific causes of MDF and MIF in samples could not be explicitly determined, the data illustrate the potential use of Hg isotopes to identify Hg sources and important atmospheric processes. In the future it will be critical to collect large-volume event-based precipitation samples for isotopic analysis so that source identification techniques currently applied to event samples can be applied to Hg isotopic measurements. In contrast to the suggestions of previous studies, ambient vapor-phase samples collected during this study displayed slightly negative or insignificant MIF while precipitation was characterized by positive MIF. Although aqueous photoreduction is a potential source of atmospheric Hg^0 in the Great Lakes, the high density of industrial point sources and the range of atmospheric redox reactions could also contribute to Hg isotopic fractionation in atmospheric samples. Therefore, conclusions obtained upon the basis of application of the limited Hg isotope data to regional or global Hg budgets or mass balance studies should be viewed with great caution until the processes that result in atmospheric Hg fractionation are better understood.

Acknowledgments

Funding for L.E.G. was provided by the Great Lakes Commission Great Lakes Atmospheric Deposition Program and the State of Illinois Environmental Protection Agency. Funding for Hg isotope laboratory analysis was provided by the University of Michigan MacArthur Professorship to J. D.B. We thank the staff and students of the University of Michigan Air Quality Laboratory and the Biogeochemistry and Environmental Isotope Geochemistry Laboratory for assistance with field supply preparation, sample processing and analysis, and thoughtful discussions. We especially thank Jim Barres for his aid in developing sampling methods and Marcus Johnson for his support in analytical method development and sample analysis. We thank four anonymous reviewers for their thoughtful comments and suggestions.

Supporting Information Available

Sample data tables, a map of measurement locations, and discussion of procedural standards. This material is available free of charge via the Internet at http://pubs.acs.org.

Literature Cited

(1) U.S. Environmental Protection Agency. *Mercury Study Report to Congress*; EPA-452/R-97-003; U.S. EPA Office of Air Quality Planning and Standards, Office of Research and Development: Washington DC, 1997; Vol. 2.
(2) Schroeder, W. H.; Munthe, J. Atmospheric mercury—An overview. *Atmos. Environ.* **1998**, *32*, 809–822.
(3) Slemr, F.; Schuster, G.; Seiler, W. Distribution, speciation, and budget of atmospheric mercury. *J. Atmos. Chem.* **1985**, *3*, 407–434.
(4) Lin, C.; Pehkonen, S. O. The chemistry of atmospheric mercury. *Atmos. Environ.* **1999**, *33*, 2067–2079.
(5) White, E. M.; Keeler, G. J.; Landis, M. S. Spatial variability of mercury wet deposition in Eastern Ohio: Summertime meteorological case study analysis of local source influences. *Environ. Sci. Technol.* **2009**, *43*, 4946–4953.
(6) Kritee, K.; Blum, J. D.; Johnson, M. W.; Bergquist, B. A.; Barkay, T. Mercury stable isotope fractionation during reduction of Hg(II) to Hg(0) by mercury resistant microorganisms. *Environ. Sci. Technol.* **2007**, *41*, 1889–1895.
(7) Kritee, K.; Blum, J. D.; Barkay, T. Mercury stable isotope fractionation during reduction of Hg(II) by different microbial pathways. *Environ. Sci. Technol.* **2008**, *42*, 9171–9177.
(8) Bergquist, B. A.; Blum, J. D. Mass-dependent and mass-independent fractionation of Hg isotopes by photoreduction in aquatic systems. *Science* **2007**, *318*, 417–420.

(9) Hintelmann, H.; Lu, S. High precision isotope ratio measurements of mercury isotopes in cinnabar ores using multi-collector inductively coupled plasma mass spectrometry. *Analyst* **2003**, *128*, 635–639.
(10) Smith, C. N.; Kesler, S. E.; Klaue, B.; Blum, J. D. Mercury isotope fractionation in fossil hydrothermal systems. *Geology* **2009**, *33* (10), 825–828.
(11) Sherman, L. S.; Blum, J. D.; Nordstrom, D. K.; McClesky, R. B.; Barkay, T.; Vetriani, C. Mercury isotopic composition of hydrothermal systems in the Yellowstone Plateau volcanic field and Guayamas Basin sea-floor rift. *Earth Planet. Sci. Lett.* **2009**, *279*, 86–96.
(12) Foucher, D.; Hintelmann, H. High-precision measurement of mercury isotope ratios in sediments using cold-vapor generation multi-collector inductively coupled plasma mass spectrometry. *Anal. Bioanal. Chem.* **2006**, *384*, 1470–1478.
(13) Gehrke, G. E.; Blum, J. D.; Meyers, P. A. The geochemical behavior and isotopic composition of Hg in a mid-Pleistocene western Mediterranean sapropel. *Geochim. Cosmochim. Acta* **2009**, *73*, 1651–1665.
(14) Ghosh, S.; Xu, Y.; Humayun, M.; Odom, L. Mass-independent fractionation of mercury isotopes in the environment. *Geochem. Geophys. Geosyst.* **2008**, *9* (3), Q03004.
(15) Biswas, A.; Blum, J. D.; Bergquist, B. A.; Keeler, G. J.; Zhouqing, X. Natural mercury isotope variation in coal deposits and organic soils. *Environ. Sci. Technol.* **2008**, *42*, 8303–8309.
(16) Jackson, T. A.; Whittle, D. M.; Evans, M. S.; Muir, D. C. G. Evidence for mass-independent and mass-dependent fractionation of the stable isotopes of mercury by natural processes in aquatic ecosystems. *App. Geochem.* **2008**, *23*, 547–571.
(17) Carignan, J.; Estrade, N.; Sonke, J. E.; Donard, O. F. X. Odd isotope deficits in atmospheric Hg measured in lichens. *Environ. Sci. Technol.* **2009**, *43*, 5660–5664.
(18) Sherman, L. S.; Blum, J. D.; Johnson, K. P.; Keeler, G. J.; Barres, J. A.; Douglas, T. A. Mass-independent fractionation of mercury isotopes in Arctic snow driven by sunlight. *Nature Geosci.* **2010**, *3*, 173–177.
(19) Schauble, E. A. Role of nuclear volume in driving equilibrium stable isotope fractionation of mercury, thallium, and other very heavy metals. *Geochim. Cosmochim. Acta* **2007**, *71*, 2170–2189.
(20) Estrade, N.; Carignan, J.; Sonke, J. E.; Donard, O. F. X. Mercury isotope fractionation during liquid−vapor evaporation experiments. *Geochim. Cosmochim. Acta* **2009**, *73*, 2693–2711.
(21) Turro, N. J. Influence of nuclear spin on chemical reactions: Magnetic isotope and magnetic field effects (A review). *Proc. Natl. Acad. Sci.U.S.A.* **1983**, *80*, 609–621.
(22) Buchachenko, A. L. The magnetic isotope effect: Nuclear spin control of chemical reactions. *J. Phys. Chem.* **2001**, *105* (44), 9995–10011.
(23) Buchachenko, A. L.; Ivanov, V. L.; Roznyatovskii, V. A.; Artamina, G. A.; Vorob'ev, A. Kh.; Ustynyuk, Yu. A. Magnetic isotope effect for mercury nuclei in photolysis of bis(*p*-trifluoromethylbenzyl)mercury. *Doklady Phys. Chem.* **2007**, *413*, 39–41.
(24) Bergquist, B. A.; Blum, J. D. The odds and evens of mercury isotopes: Applications of mass-dependent and mass-independent isotope fractionation. *Elements* **2009**, *5*, 353–357.
(25) Landis, M. S.; Keeler, G. J. Atmospheric mercury deposition to Lake Michigan during the Lake Michigan Mass Balance Study. *Environ. Sci. Technol.* **2002**, *36*, 4518–4524.
(26) Hammerschmidt, C. R.; Fitzgerald, W. F. Methylmercury in freshwater fish linked to atmospheric mercury deposition. *Environ. Sci. Technol.* **2006**, *40*, 7764–7770.
(27) Zambardi, T.; Sonke, J. E.; Toutain, J. P.; Sortino, F.; Shinohara, H. Mercury emissions and stable isotopic compositions at Vulcano Island (Italy). *Earth Planet. Sci. Lett.* **2009**, *277*, 236–243.
(28) Hoyer, M.; Burke, J.; Keeler, G. J. Atmospheric sources, transport and deposition of mercury in Michigan−2 years of event precipitation. *Water, Air, Soil Pollut.* **1995**, *80*, 199–208.
(29) 1999 inventory of toxic air emissions: Point, area, and mobile sources; Great Lakes Commission: Ann Arbor, MI, 1999; http://www.glc.org/air/inventory/1999/.
(30) Landis, M. S.; Vette, A. S.; Keeler, G. J. Atmospheric mercury in the Lake Michigan Basin: Influence of the Chicago/Gary urban area. *Environ. Sci. Technol.* **2002**, *36*, 4508–4517.
(31) Keeler, G. J.; Landis, M. S.; Norris, G. A.; Christianson, E. M.; Dvonch, J. T. Sources of Mercury Wet Deposition in Eastern Ohio, USA. *Environ. Sci. Technol.* **2006**, *40*, 5874–5881.
(32) Cohen, M. D.; Artz, R. S.; Draxler, R. R. *Report to Congress: Mercury Contamination in the Great Lakes*; NOAA Air Resources Laboratory: Silver Spring, MD, 2007.
(33) U.S. Environmental Protection Agency. *An Introduction to the Issues and the Ecosystems*; EPA-453/B-94/030; U.S. EPA Office of Air Quality Planning and Standards: Durham, NC, 1994.
(34) Vette, A. S.; Landis, M. S.; Keeler, G. J. Deposition and emission of gaseous mercury to and from Lake Michigan during the Lake Michigan Mass Balance Study (July, 1994−October, 1995). *Environ. Sci. Technol.* **2002**, *36*, 4525–4532.
(35) Lynam, M. M.; Keeler, G. J. Automated speciated mercury measurements in Michigan. *Environ. Sci. Technol.* **2005**, *39* (23), 9253–9262.
(36) Liu, B.; Keeler, G. J.; Dvonch, J. T.; Barres, J. A.; Lynam, M. M.; Marsik, F. J.; Taylor Morgan, J. Urban−rural differences in atmospheric mercury speciation. *Atmos. Environ.* **2010**, *44*, 2013–2023.
(37) Landis, M. S.; Keeler, G. J. Critical evaluation of a modified automatic wet-only precipitation collector for mercury and trace element determinations. *Environ. Sci. Technol.* **1997**, *31*, 2610–2615.
(38) Blum, J. D.; Bergquist, B. A. Reporting the variations in the natural isotopic composition of mercury. *Anal. Bioanal. Chem.* **2007**, *388*, 353–359.
(39) Hower, J. C.; Thomas, G. A.; Palmer, J. Impact of the conversion to low-NOx combustion on ash characteristics in a utility boiler burning Western US coal. *Fuel Process. Technol.* **1999**, *61*, 175–195.
(40) Freme, F. U.S. Coal Supply and Demand: 2008 Review; U.S. Department of Energy, Energy Information Administration; http://www.eia.doe.gov/cneaf/coal/page/special/article_dc.pdf.
(41) Draxler, R. R.; Hess, G. D. An overview of the HYSPLIT_4 modelling system for trajectories, dispersion and deposition. *Aust. Met. Mag.* **1998**, *47*, 295–308.
(42) Clean Air Status and Trends Network (CASTNET); http://www.epa.gov/castnet/.
(43) National Climatic Data Center, Local Climatological Data Publication; http://www7.ncdc.noaa.gov/IPS/lcd/lcd.html.
(44) Dvonch, J. T.; Graney, J. R.; Marsik, F. J.; Keeler, G. J.; Stevens, R. K. An investigation of source−receptor relationships for mercury in south Florida using event precipitation data. *Sci. Total Environ.* **1998**, *213*, 95–108.
(45) Dvonch, J. T.; Graney, J. R.; Keeler, G. J.; Stevens, R. K. Use of elemental tracers to source apportion mercury in South Florida precipitation. *Environ. Sci. Technol.* **1999**, *33*, 4522–4527.
(46) Gratz, L. E.; Keeler, G. J.; Miller, E. K. Long-term relationships between mercury wet deposition and meteorology. *Atmos. Environ.* **2009**, *43*, 6218–6229.
(47) Zheng, W.; Hintelmann, H. Mercury isotope fractionation during photoreduction in natural water is controlled by its Hg/DOC ratio. *Geochim. Cosmochim. Acta* **2009**, *73*, 6704–6715.
(48) Munthe, J. The aqueous oxidation of elemental mercury by ozone. *Atmos. Environ.* **1992**, *26A*, 1461–1468.
(49) Lin, C.; Pehkonen, S. O. Aqueous free-radical chemistry of mercury in the presence of iron oxides and ambient aerosol. *Atmos. Environ.* **1997**, *31*, 4125–4137.
(50) Hynes, A. J.; Donohue, D. L.; Goodsite, M. E.; Hedgecock, I. M. Our current understanding of major chemical and physical processes affecting mercury dynamics in the atmosphere and at the air−water/terrestrial interfaces. In *Mercury Fate and Transport in the Global Atmosphere*; Pirrone, N., Mason, R., Eds; Springer Science + Business Media: New York, 2009; pp 427−457.
(51) Munthe, J.; Xiao, Z. F.; Lindqvist, O. The aqueous reduction of divalent mercury by sulfite. *Water, Air, Soil Pollut.* **1991**, *56*, 621–630.
(52) Seigneur, S.; Wrobel, J.; Constantinou, E. A chemical kinetic mechanism for atmospheric inorganic mercury. *Environ. Sci. Technol.* **1994**, *28*, 1589–1597.
(53) Lohman, K.; Seigneur, C.; Edgerton, E.; Jansen, J. Modeling mercury in power plant plumes. *Environ. Sci. Technol.* **2006**, *40*, 3848–3854.
(54) Lindberg, S. E.; Brooks, S.; Lin, C.-J.; Scott, K. J.; Landis, M. S.; Stevens, R. K.; Goodsite, M.; Richter, A. Dynamic oxidation of gaseous mercury in the arctic troposphere at polar sunrise. *Environ. Sci. Technol.* **2002**, *36*, 1245–1256.
(55) Tackett, P. J.; Cavender, A. E.; Keil, A. D.; Shepson, P. B.; Bottenheim, J. W.; Morin, S.; Deary, J.; Steffen, A.; Doerge, C. A study of the vertical scale of halogen chemistry in the Arctic troposphere during polar sunrise at Barrow, Alaska. *J. Geophys. Res.* **2007**, *112*, D07306.

(56) Hedgecock, I. M.; Pirrone, N. Mercury and photochemistry in the marine boundary layer-modeling studies suggest the in situ production of reactive gas phase mercury. *Atmos. Environ.* **2001**, *35*, 3055–3062.
(57) Lin, C.; Pongprueska, P.; Lindberg, S. E.; Pehkonen, S. O.; Byun, D.; Jang, C. Scientific uncertainties in atmospheric mercury models I: Model science evaluation. *Atmos. Environ.* **2006**, *40*, 2911–2928.
(58) Dye, T. S.; Roberts, P. T.; Korc, M. E. Observations of transport processes for ozone and ozone precursors during the 1991 Lake Michigan Ozone Study. *J. App. Met.* **1995**, *34*, 1877–1889.
(59) Munthe, J.; McElroy, W. J. Some aqueous reactions of potential importance in the atmospheric chemistry of mercury. *Atmos. Environ.* **1992**, *26A*, 553–557.
(60) Carpi, A. Mercury from combustion sources: A review of the chemical species emitted and their transport in the atmosphere. *Water, Air, Soil Pollut.* **1997**, *98*, 241–254.
(61) Kesselmeier, J.; Staudt, M. Biogenic volatile organic compounds (VOC): An overview on emission, physiology and ecology. *J. Atmos. Chem.* **1999**, *33*, 23–88.
(62) Willey, J. D.; Kieber, R. J.; Eyman, M. S.; Avery, G. B. Rainwater dissolved organic carbon: Concentrations and global flux. *Global Biogeochem. Cycles* **2000**, *14* (1), 139–148.
(63) Mead, C.; Anbar, A. D.; Johnson, T. M. *Mass-independent fractionation of Hg isotopes resulting from photochemical self shielding*; Goldschmidt: Knoxville, TN, 2010.

ES100383W